BILINGUAL PUBLISHING CO.
Pioneer of Global Academics Since 1984

Journal of Geological Research
https://ojs.bilpublishing.com/index.php/jgr-a

ARTICLE

Interpretation of Aeromagnetic Data of Part of Gwagwalada Abuja Nigeria for Potential Mineral Targets

Priscillia Egbelehulu* Abu Mallam Abel. U. Osagie

Department of Physics, University of Abuja, Abuja, Nigeria

ARTICLE INFO

Article history
Received: 16 August 2021
Revised: 12 September 2021
Accepted: 14 September 2021
Published Online: 30 September 2021

Keywords:
Aeromagnetic
Lineament
Faults
Total magnetic intensity

ABSTRACT

This study analyzes aeromagnetic data over a section of Gwagwalada in Abuja. The data were obtained from the Nigerian Geological Survey Agency acquired at 100 m terrain clearance. The study area spans longitudes 7.0875 E to 7.1458 E and latitude 8.9625 N to 9.0 N (about 27 km2). The dataset was reduced to the equator (RTE) and downward continued by 50 m. Analytic signal filter was applied on TMI-RTE grid to detect the edges of the magnetic bodies present. The structure was observed to trend NE-SW. The CET lineament map reveals intersections such as junctions and corners on the map. This revealed structure liable for potential mineralization zone. Euler deconvolution technique applied over the transformed dataset ascertain the location and depth of the structure, having a maximum depth of about 421 m and a minimum of about 59 m. Variation in magnetic depth and susceptibility contrast is specified by the gridded SPI depth map.

1. Introduction

Minerals are usually deposited underneath the earth surface. Detecting them to a great extent depends on the characteristics or properties they possess which distinguish them from their surrounding media.

Geophysical method assumed for their survey depends on their properties [4].

Magnetic method plays a vital role in mineral exploration. Its importance is seen in its ability to delineate structures like faults, folds, contacts, shear zones, intrusions and detection of favorable areas of ore deposits [1]. It responds to ferromagnetic materials and detects metallic objects [11]. It is concerned with the measurement of the intensity of the earth's magnetic field.

Earth's magnetic field anomalies are usually a result of either induced or remanent magnetism, due to secondary magnetization which is induced in a ferrous body by the earth's magnetic field. The shape, dimension, and amplitude of an induced magnetic anomaly are functions of the kind of orientation, geometry, size, depth, intensity, inclination of the earth's magnetic field in the area of interest and magnetic susceptibility of the body [3].

Most magnetic rocks are known to contain several combinations of induced and remanent magnetization which affects the earth's primary field [10]. The magnitudes

*Corresponding Author:
Priscillia Egbelehulu,
Department of Physics, University of Abuja, Abuja, Nigeria;
Email: priscilliaegbelehulu@gmail.com

DOI: https://doi.org/10.30564/jgr.v3i4.3581

of these fields depend largely on the quantity, size of magnetic-mineral grains and their composition. Magnetic anomalies could be linked to primary igneous or sedimentary processes that build the magnetic mineralogy. They could also be as a result of secondary alteration that introduces or removes magnetic minerals.

The results of any geophysical survey are used to identify a target of interest, or to correlate the spatial variation of values of the rock property with variations in the geology. Thus, survey helps to get valuable information on the geology and possibly to find targets of economic interest and importance in the study area [13]. Understanding the nature of the mineralization and how it originates is an important factor in mining exploration, since minerals are structurally controlled and are associated with faults, fractures and shear zones. Delineating these structures aids future exploration, giving an idea of the mining potential of the region. This research aims at interpreting aeromagnetic data for potential mineral target.

Objectives of the study are

•To identify lineaments.

•To delineate geological structures that might host possible minerals.

•To ascertain the depth of the vein.

2. Location

The area of study is located in Abuja, Gwagwalada area council (Figure 2). It is about 55 km from the capital city (Abuja). It is bounded by 7.0875 E to 7.1458 E and latitude 8.9625 N to 9.0 N, which covers 27 km^2 north-eastern part of Gwagwalada. The contour obtained from the topographic map of the study area is used to produce a digital terrain model of the area (Figure 1) using The Generic Mapping Tools (GMT) software. This gives an idea about the geomorphology of the area. The area is located within the broken-line rectangular box is a low land terrain with hills located at the northeastern and central part with a height of about 400 m above sea level with valleys observed along the hills.

2.1 Geology of the Study Area

The geology of the Federal Capital Territory (FCT), Abuja is underlain by two major rock formations - the Basement Complex and sedimentary rock formations [8]. The dominant rock within the study area is banded gneisses. The outcrops are well foliated showing prominent gneissosity with the alternation of bands of mafic and felsic minerals. They are medium-to coarse-grained with large quartz intrusions exploiting joints and weak zones within the rock.

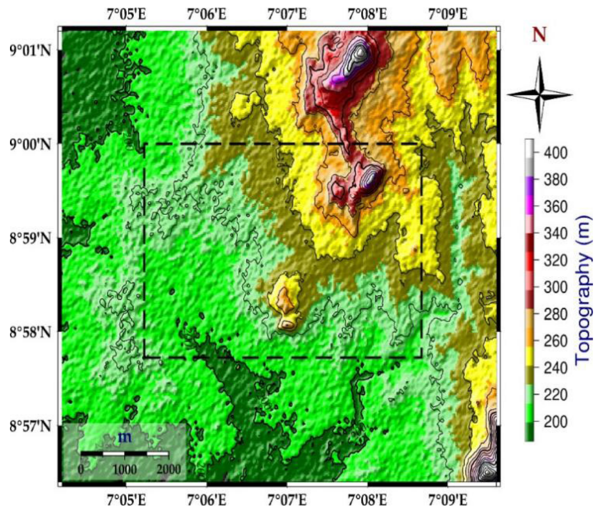

Figure 1. Topographic Map of Study Area

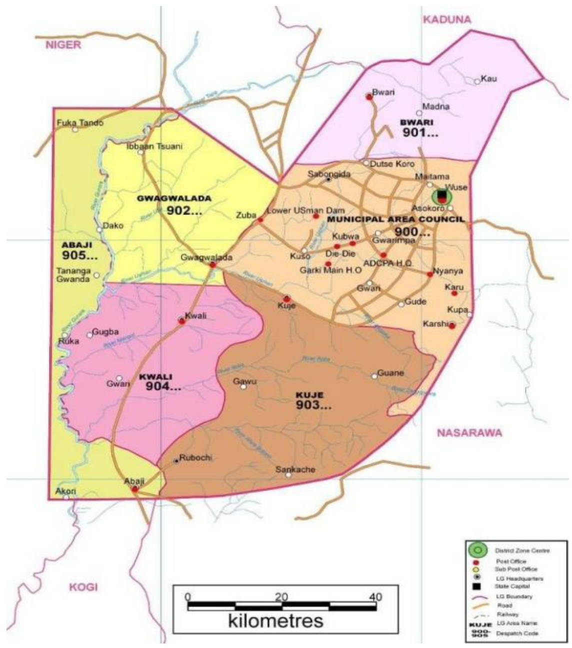

Figure 2. Location Map of Study Area

3. Materials and Method

The major component of the study involves image enhancement of the aeromagnetic dataset acquired from the Nigerian Geological Survey Agency (NGSA). The magnetic anomalies associated with local magnetic variations of the study area was obtained by the removal of the normal geomagnetic field that is, by subtracting 33000nT from the dataset. The International Geomagnetic Reference Field (IGRF) formula [2] which was computed by GEOMAG program is used for the reduction. The dataset is interpolated by employing the minimum curvature gridding algorithm obtainable in the Geosoft Oasis Montaj 8.4 software. The angle of inclination and declination was taken at -6.4° and -1.7° respectively. These values were acquired from the eleventh generation international geomagnetic Reference Field (IGRF) formula [2] at latitude 8o59'N and longitude 7o07'E around the mid-point of the region. The map is also characterized by magnetic highs trending NE-SW. This configuration could be ascribed to a relatively deep-seated low relief basement structures with the igneous rocks composition. On the reduced to equator (RTE) map, analytic signal, centre for exploration targeting (CET), Euler deconvolution and Source parameter imaging (SPI) was applied over the dataset.

3.1 Analytic Signal

Analytic Signal method is used for detecting the edges of magnetic bodies. The conceptualization of analytic signal for magnetic data interpretation was initially introduced [6]. It reveals that amplitude yields a bell-shaped function over every corner of a 2D body with polygonal cross-section. For a remote corner, the maximum of the bell-shaped curve is detected precisely over the corner. At half its maximum amplitude, the width of the curve is equal to twice the depth to the corner. However, resolving for these parameters is not affected by the presence of the remanent magnetization. Horizontal locations are usually well verified by this method nonetheless depth determinations are only valid for polyhedral bodies [7]. The 3D analytic signal was employed to approximately estimate positions of magnetic contacts and acquire depth estimates from gridded data [12].

3.2 Center of Exploration Targeting (CET)

The CET grid analysis examines the texture of a laterally continuous line-like region of discontinuity such as lineament along ridges and edges as well as areas of deviation to locate deposit occurrence favorability.

3.3 Euler Deconvolution

This technique uses the first-order x, y and z derivatives to determine the location and the depth for different idealized targets (sphere, cylinder, thin dike, and contact). Every single one of them can be characterized by a specific structural index. Eigen values generated in Euler solution could be further analyzed to decide whether an individual anomaly was 2D or 3D.

$$X\frac{\partial T}{\partial x}+Y\frac{\partial T}{\partial y}+Z\frac{\partial T}{\partial z}+NT=x_0\frac{\partial T}{\partial x}+y_0\frac{\partial T}{\partial y}+z_0\frac{\partial T}{\partial z}+NB \quad (1)$$

Where;

x_0, y_0, z_0 *are coordinate of magnetic force.*

$\frac{\partial T}{\partial x}, \frac{\partial T}{\partial y}, \frac{\partial T}{\partial z}$ *are derviatives of total field with respect to x, y, z*

N-Structural Index (SI) helps relates rate of change of a potential field with distance.

B-It's a local background representing the "regional" field within a sliding window with an adjustable size [5]. The SI to a great extent depends on the type and physical parameters of the potential field this provides an excellent overview of the Euler's homogeneity equation properties in general and the SI in particular [15].

Estimating depth by applying Euler deconvolution technique helps in delineating geologic contacts where faults usually occur. This technique provides an automated estimation of the source location and depth. Thus, it is used as a boundary finder as well as a depth estimator. It is often deployed in magnetic interpretation due to its uniqueness-since it requires only a little precedent knowledge about the magnetic source geometry, and it requires no information about the magnetization vector [9] and [16].

3.4 Source Parameter Imaging

This technique was developed due to complex analytic signal. SPI is occasionally referred to as the local wave number method [17-19]. It has its maxima located over isolated contacts, and its depths is estimated without the presumption of the thickness of the source bodies [14]. Solution grids obtained from the SPI™ technique shows edge locations, depths, dips and susceptibility contrasts. The local wave number maps more closely similar geology compared to magnetic map or its derivatives.

4. Results and Discussion

The total magnetic intensity (TMI) grid Figure 3a is reduced to the equator Figure 3b. This ensures that the magnetic anomaly is directly positioned on the body causing them since the direction of magnetization varies. The magnetic signature is enhanced and trends in NE-SW direction of the study area.

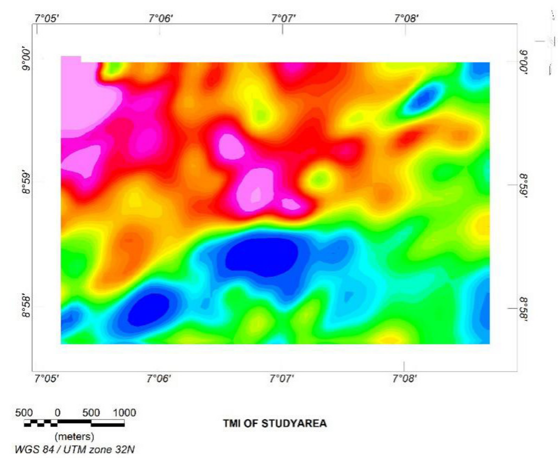

Figure 3a. TMI map of Study area

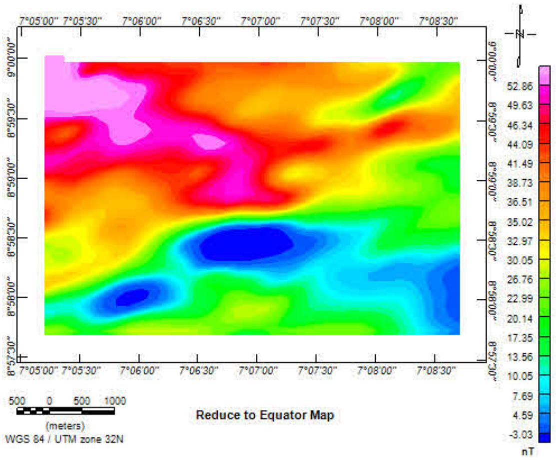

Figure 3b. TMI map reduce to Equator

4.2 Structural Analysis from Analytic Signal Plug

It is characterized with high and low amplitude thereby separating regions of outcrop and sedimentation. Since the result is amplitude domain, regions possessing outcrops have a significantly high amplitude shown in Figure 4 with red and pink color and areas having low amplitude identified with blue coloration. Analytic signal is more discontinuous than the simple horizontal gradient because a maximum generated directly over the discrete bodies along their edges.

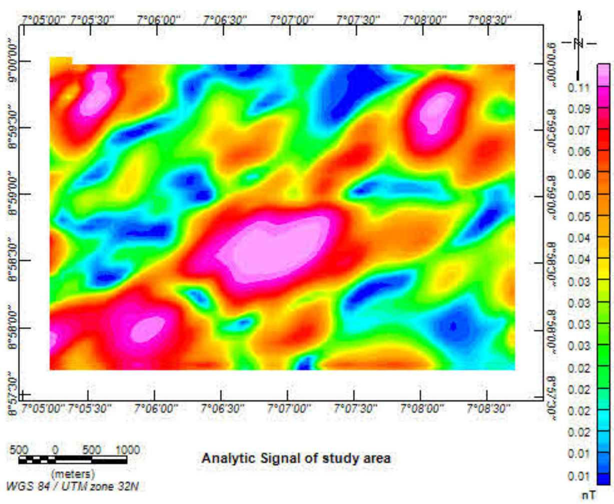

Figure 4. Analytical Map of Study Area

4.3 Application of Center of Exploration Targeting (CET) Grid Analysis and Results

CET grid analysis is applied to RTE grid so that anomalies are shifted over their causative structures. Standard deviation and phase symmetry plug-in was applied to produce the map in Figure 5a, while application of the amplitude threshing and the skeleton to vector plug-in yielded map Figure 5b. Form Figure 5a it can be deduced that the area shown in blue coloration represent areas with very low amplitudes are due to a deeper magnetic sources. The region is observed to follow NE-SW trends, which coincides with the trending of the area. The areas depicted by the pink colour are the outcrop of migmatitic-gneiss, which is the most abundant of the basement rock in the area. Rocks of lithological group of the basement complex also identified in the area are banded- gneiss (Biotite-gneiss), granite-gneiss and quartz veins which were observed at the northeastern part of the map, northwest, central part and the southwestern part of the map all trending NE-SW as shown in Figure 1. Figure 5b, which is the CET lineament reveals positions of selected intersections such as junctions and corners of the detected segmented lines. Areas where the line structure intercept or change direction are regarded as high mineralization areas.

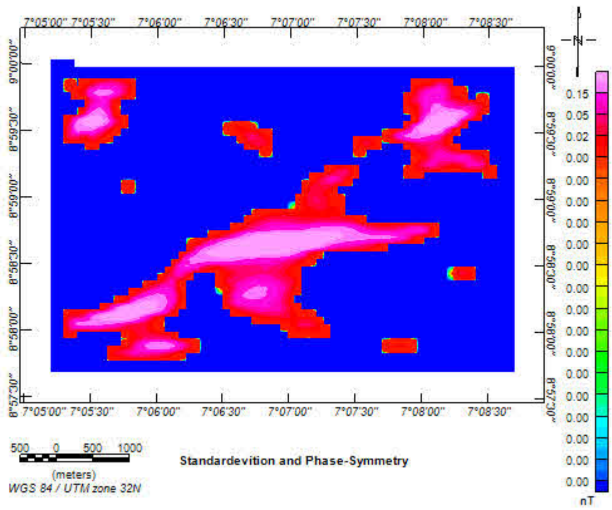

Figure 5a. Standard Deviation and Phase Symmetry Map of the Study Area

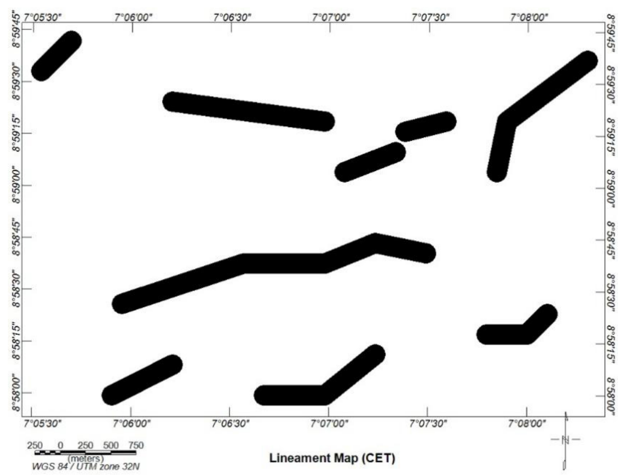

Figure 5b. Lineament Map (CET) of the Study Area

4.4 Application of Euler Deconvolution for Structural Analysis and Result

Euler deconvolution was carried out on the RTE. Its method for depth estimation is an automated technique used in detecting the source of potential field base on the amplitude and gradients. Structural index (SI) and window sizes are selected appropriately as (dyke =1) Figure 6. Euler deconvolution explore the area to locate structures and estimate the depth to which the structures exists. To achieve the best SI, structural indices were taken as 1.

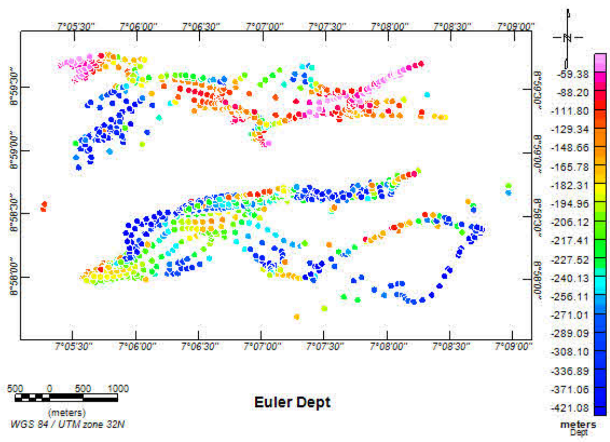

Figure 6. Euler Deconvolution of the study Area

Depth estimated in the west (W) to the East (E), Northeast (NE) and Northwest (NW) direction over the major anomaly decreases gradually. The pink circles represent the depths of the main anomaly having a depth about 59.38 m depth of the extrusive body (blue circles) which is about 421.08 m is different from the main anomaly. The degree of accuracy of Euler depth depends on the structures or on the anomaly falling on the center of the window.

4.5 Application of Source Parameter Imaging and Results

SPI method makes easier interpretation of magnetic data significantly Figure 7. Variation in magnetic depth and susceptibility dissimilarity within the study area is usually indicated by the gridded SPI map and colour legend. The negative values in the legend indicate depth of magnetic bodies, which could be deep-seated crystalline rocks or a shallow intrusion. The Pink coloration indicates area associated with near surface magnetic bodies with depth approximately 99.13 m, while the blue colour indicates area of deep seated magnetic bodies having a depth ranging from 246.71 m to 408.76 m. SPI depth ranges generally from 99.13 m (near surface depth) to 408.76 m (deep seated magnetic bodies).

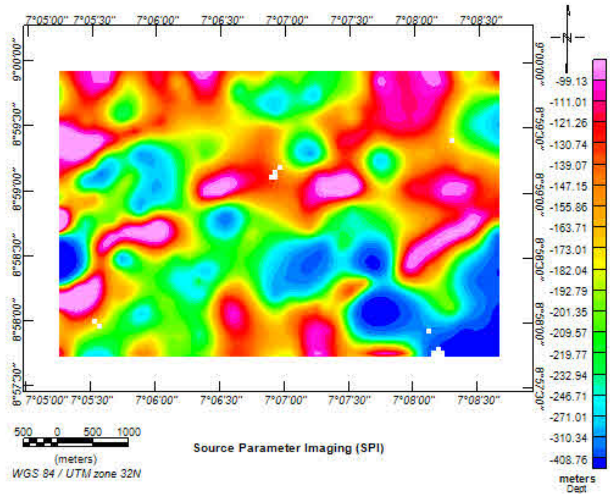

Figure 7. SPI Map of the Study Area

5. Conclusions

Analytical signal filter map Figure 4 is discontinuous and shows a prominent NE-SW trend. However, a maximum is generated directly over separate bodies alongside their edges. The maximum indicates contact depth with the condition that the signal originating from a single contact was obtained. Euler deconvolution plug-in was applied and obtained depth of the source potential field based on the amplitude and gradient. The depth of the main anomaly was 59.38 m. The center for exploration targeting (CET) plug-in applied on the RTE grid clearly revealed that the CET analysis was extremely effectual and useful in identifying the occurrence, location of favorable mineralization area and tracing the structural lineament. Which were traced to longitude 7005’30’’, 70 07’00’’, 70 08’00” and latitude 8059’32’’, 8058’45’’, 8059’15’’ also coincide with feature in Euler deconvolution (depth). Finally, source parameter imaging (SPI) Figure 7 applied using a pre-processing grid of horizontal and vertical derivative, indicated variation in magnetic depth and susceptibility contrast within the study area.

References

[1] Elkhateeb, O.S. Delineation Potential Gold Mineralization Zone in A Part of Central Eastern Desert, Egypt Using Airborn Magnetic and Radiometric data [J]. *NRIAG Journal of Astronomy and Geophysics* (2018). 55-70.

[2] Finlay C.C, Maus S, Beggan C.D, Bondar T.N, Chambodut A, Chernova T.A, Chulliat A, Golovkov V.P, Hamilton B, Hamoudi M, Holme R. International geomagnetic reference field: the eleventh generation [J]. Geophysical Journal International (2010).

183(3):1216-30.

[3] Hinze W.J. The role of gravity and magnetic methods in engineering and environmental studies. InGeotechnical an Environmental Geophysics: Volume I: Review and Tutorial [J]. Society of Exploration Geophysicists (1990). 75-126.

[4] Kearey, P, Brooks, M., & Ian, H. An Introduction to Geophyscial Exploration. Third Edition Blackwell Publishing (2002).

[5] Mushayandebvu M.F, Lesur V, Reid A.B, Fairhead J.D. Grid Euler deconvolution with constraints for 2D structures [J]. Geophysics (2004). 69(2):489-96.

[6] Nabighian, M. N. The analytic signal of two-dimensional magnetic bodies with polygonal cross-section - Its properties and use for automated anomaly interpretation [J]. Geophysics (1972), 37, 507-517.

[7] Nabighian, M. N. Additional comments on the analytic signal of two-dimensional magnetic bodies with polygonal cross-section [J] Geophysics (1974), 39, 85-92.

[8] Offodile, M. E. The development and management of groundwater in Nigeria. *Contributions of Geosciences and Mining to National Development, (NMGS)* (2003), 1-7.

[9] Reid, A.B., Allsop, J.M., Granser, H., Millett, A.J., Somerton, I.W. Magnetic Interpretation in Three Dimension Using Euler Deconvolution [J]. *Geophysics* (1990), 55, 80-90.

[10] Reynolds, R.L., Rosenbaum, J.G., Hudson, M.R and Fishman, N.S Rock Magnetism, the Distribution of Magnetic Minerals in Earth Crust and Aeromagnetic Anomalies. U.S Geological Survey Bulletin (1990). 24-45.

[11] Robert, J.H. Application of Magnetic and Electromagnetic Methods to Locate Buried Metal. U.S Department of Interior, U.S Geological Survey, Open-File Report (2003). 03-317.

[12] Roest, W.R., Verhoef, J., and Pilkington, M. Magnetic interpretation using the 3-D analytic signal. *Geophysics* (1992), 57, 116-125.

[13] Scott, W.J Geophysics for Mineral Exploration-A Manual for Prospectors (2014). 1-2, 11-14.

[14] Smith, R.S., Thurston, J.B., Dai, Ting-Fan, and MacLeod, I.N. SPI™ - the improved source parameter imaging method: Geophysical Prospecting (1998), 46, 141-151.

[15] Stavrev, P. and Reid, A. Degrees of Homogeneity of Potential Fields and Structural Indices of Euler Deconvolution [J]. *Geophysics* (2007), 72, 1-12.

[16] Thompson, D.T. A New Technique of Making Computer Assisted Depth Estimates from Magnetic Data [J]. Geophysics (1982), 47: 31-37.

[17] Thurston, J. B., Smith, R. S. and Guillon, J-C. A multimodel method for depth estimation from magnetic data [J]. Geophysics (2002), 67, 555-561.

[18] Thurston, J., Guillon, J. -C. and Smith, R. Model-independent depth estimation with the SPI™ method: SEG Expanded Abstracts (1999), 18,403-406.

[19] Thurston, J.B., and Smith, R.S. Automatic conversion of magnetic data to depth, dip, and susceptibility contrast using the SPI™ method: Geophysics (1997), 62, 807-813.